Electrochemical and Functional Characterization of the Proline Dehydrogenase Domain of the PutA Flavoprotein from *Escherichia coli*†

Madhavan P. Vinod, Padmanetra Bellur, and Donald F. Becker*

Department of Chemistry and Biochemistry, University of Missouri—St. Louis, St. Louis, Missouri 63121

Received February 20, 2002

ABSTRACT: The multifunctional PutA flavoprotein from *Escherichia coli* is a peripherally membrane-bound enzyme that has both proline dehydrogenase (PDH) and Δ^1-pyrroline-5-carboxylate dehydrogenase (P5CDH) activities. In addition to its enzymatic functions, PutA displays DNA-binding activity and represses proline catabolism by binding to the control region DNA of the *put* regulon (*put* intergenic DNA). Presently, information on structure−function relationships for PutA is derived from primary structure analysis. To gain further insight into the functional organization of PutA, our objective is to dissect PutA into different domains and to characterize them separately. Here, we report the characterization of a bifunctional proline dehydrogenase ($PutA_{669}$) that contains residues 1−669 of the PutA protein. $PutA_{669}$ purifies as a dimer and has a PDH specific activity that is 4-fold higher than that of PutA. As anticipated, $PutA_{669}$ lacks P5CDH activity. At pH 7.5, an E_m (E−FAD/E−FADH$^-$) of −0.091 V for the two-electron reduction of $PutA_{669}$-bound FAD was determined by potentiometric titrations, which is 15 mV more negative than the E_m for PutA-bound FAD. The pH behavior of the E_m for $PutA_{669}$-bound FAD was measured in the pH range 6.5−9.0 at 25 °C and exhibited a 0.03 V/pH unit slope. Analysis of the DNA and membrane-binding properties of $PutA_{669}$ shows that it binds specifically to the *put* intergenic control DNA with a binding affinity similar to that of PutA. In contrast, we did not observe functional association of $PutA_{669}$ with membrane vesicles. We conclude that $PutA_{669}$ has FAD-binding and DNA-binding properties comparable to those of PutA but lacks a membrane-binding domain necessary for stable association with the membrane.

Escherichia coli and *Salmonella typhimurium* combine proline dehydrogenase (PDH,[1] EC 1.5.99.8) and Δ^1-pyrroline-5-carboxylate dehydrogenase (P5CDH, EC 1.5.1.12) activities onto the single polypeptide, PutA, which is encoded by the *putA* gene (*1*−*3*). Isolation and analysis of the *putA* gene from other bacteria such as *Klebsiella pneumoniae*, *Rhodobacter capsulatus*, *Pseudomonas putida*, *Bradyrhizobium japonicum*, and *Sinorhizobium meliloti* show that PutA is also a bifunctional enzyme in these nitrogen-fixing microorganisms (*4*−*8*). PutA is a peripherally membrane-bound dehydrogenase that catalyzes the 4e$^-$ oxidation of L-proline to glutamate in two successive steps (*3*, *9*−*12*). The PDH domain of PutA performs the first step of proline oxidation by catalyzing the flavin-dependent dehydrogenation of proline, which involves two half-reactions. In the reductive half-reaction, two electrons, presumable as a hydride, are transferred from proline to the noncovalently bound flavin

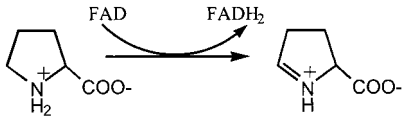

adenine dinucleotide (FAD) to generate Δ^1-pyrroline-5-carboxylate (P5C). In the oxidative half-reaction, PutA associates peripherally with the membrane where the PDH domain catalyzes the transfer of two electrons from reduced FAD to an acceptor in the electron-transport chain (*9*, *13*). Next, P5C is hydrolyzed to yield γ-glutamic acid semialdehyde. Presently, it is not known whether PutA catalyzes a Schiff base hydrolysis of P5C to γ-glutamic acid semialdehyde or if it occurs spontaneously. The P5CDH domain of PutA then performs the second step of proline oxidation by catalyzing the NAD-dependent oxidation of γ-glutamic acid semialdehyde to glutamate. Steady-state kinetic studies

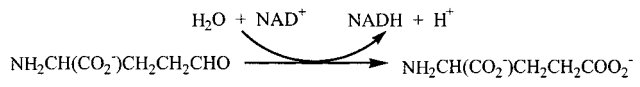

indicate that PutA shuttles P5C from the PDH active site to the P5CDH active site via a substrate channel, thus improving the efficacy of proline conversion to glutamate (*14*).

In addition to its enzymatic functions, PutA is an autogenous transcriptional regulator of the proline utilization (*put*) regulon, which encodes the *putP* and *putA* genes (*1*, *12*, *15*−*18*). The *putP* gene product is a high-affinity Na^+/proline

† We gratefully acknowledge the financial support of the University of Missouri—St. Louis Chemistry and Biochemistry Department, Research Corp. (Award RI0384), National Science Foundation (MCB0091664), National Institutes of Health (GM61068), and ACS-PRF (36470-G4).

* Address correspondence to this author. Phone: 314-516-7345. Fax: 314-516-5342. E-mail: chedbeck@jinx.umsl.edu.

[1] Abbreviations: FAD, flavin adenine dinucleotide; *put*, proline utilization; NAD^+, nicotinamide adenine dinucleotide; PDH, proline dehydrogenase; P5CDH, Δ^1-pyrroline-5-carboxylate dehydrogenase, P5C, Δ^1-pyrroline-5-carboxylate; DCPIP, dichlorophenolindophenol; EDTA, ethylenediaminetetraacetic acid; MOPS, 3-(*N*-morpholino)-propanesulfonic acid; E_m, reduction potential.

10.1021/bi025706f CCC: $22.00 © 2002 American Chemical Society
Published on Web 04/25/2002

transporter (*19*). PutA is known to be a transcriptional repressor of the *put* regulon in *E. coli*, *S. typhimurium*, *K. pneumoniae*, *R. capsulatus*, *P. putida*, and *S. meliloti* (*4*−*6*, *12*, *20*, *21*). PutA is part of an emerging class of bacterial enzymes that combine enzymatic and DNA-binding activities on a single polypeptide. Other multifunctional transcriptional regulators include PepA from *E. coli*, which is a repressor of the *carAB* operon, and NadR from *S. typhimurium*, which is a repressor of the NAD biosynthesis genes (*22*−*24*). PutA regulation of the *put* regulon is dependent on the availability of proline. The *putP* and *putA* genes are transcribed in opposite directions from the *put* intergenic control region. In the absence of proline, PutA binds to promoter sequences in the *put* intergenic region and represses the divergent transcription of the *putP* and *putA* genes (*12*, *20*). In the presence of proline, PutA changes its intracellular location by peripherally associating with the membrane (*11*, *13*, *18*, *25*). Thus, transcription of the *put* regulon is activated by translocation of PutA from the cytoplasm to the membrane. The mechanism for how PutA changes its intracellular location is not known. However, because PutA binding to the *put* intergenic DNA is not significantly influenced by proline or electrochemical reduction of FAD, it appears that changes in PutA−membrane interactions are critical for directing PutA intracellular location and function (*12*, *26*, *27*).

E. coli PutA is comprised of 1320 amino acids, which provides a large structural scaffold to support its enzymatic and DNA-binding activities (*28*). Presently, structure−function information for PutA is derived from sequence comparisons of PutA with other organisms. Upon sequencing the *putA* gene from *E. coli*, Ling et al. (1994) performed primary structural analysis with discrete PDH and P5CDH enzymes to locate the PDH and P5CDH domains in PutA (*28*). In eukaryotes, PDH and P5CDH are distinct mitochondrial enzymes that are encoded by two separate genes. Sequence comparisons of PutA with PDH from *Saccharomyces cerevisiae* (*PUT1*) and *Drosophila melanogaster* (*slgA*) revealed that the PDH domain is located approximately in residues 340−590 of PutA (*28*). The FAD-binding motif was postulated to be in residues 315−357 since they are similar to the consensus FAD-binding region in succinate dehydrogenase. Sequence analysis of PutA with P5CDH from *S. cerevisiae* (*PUT2*) revealed the P5CDH domain in PutA is comprised of residues 650−1130 (*28*). Homology was also found between residues 650−1100 of PutA and mammalian aldehyde dehydrogenases. Possible NAD-binding sites in PutA were located by identifying sequence patterns that typically comprise adenine dinucleotide binding sites. A GxGxxG motif was found at residues 1090−1095 and a GxGxxxG motif was found at residues 833−839, 1045−1051, and 1095−1101. The DNA-binding and membrane-binding domains of PutA, however, have not yet been identified since no primary structural homologues are known.

The objective of this work was to isolate and separately characterize the PDH domain of PutA to gain further insights into the functional organization and regulatory mechanism of PutA. On the basis of the primary structure analysis of PutA, we genetically engineered a recombinant PDH by separating the PDH and P5CDH domains in PutA. We now report the electrochemical and functional properties of a truncated PutA protein from *E. coli* that contains amino acid residues 1−669 ($PutA_{669}$). As anticipated from the sequence alignment predictions, $PutA_{669}$ contains PDH activity but is devoid of P5CDH activity. The redox properties of FAD bound to $PutA_{669}$ establish that $PutA_{669}$ binds FAD similarly to PutA. We also demonstrate that $PutA_{669}$ binds specifically to the *put* intergenic control DNA and therefore is a bifunctional PDH. Recently, crystals of $PutA_{669}$ were obtained which diffract to 2.2 Å resolution (*29*). Thus, we anticipate coupling the functional data obtained in this study with the three-dimensional structure of $PutA_{669}$ to identify key structure−function relationships in PutA.

MATERIALS AND METHODS

Enzymes and Chemicals. All chemicals and buffers were purchased from Fisher or Sigma-Aldrich Inc. DL-P5C was synthesized and quantitated using *o*-aminobenzaldehyde as previously described by Strecker (*30*). Pyocyanine was prepared by photooxidation of phenazine methosulfate. Taq DNA polymerase and ϕX174 ladder DNA were purchased from Promega. Protein standards for size exclusion chromatography were purchased from Sigma. Purified full-length PutA protein was prepared as previously described (*27*). All experiments used NanoPure water.

Bacterial Strains, Plasmids, and put Intergenic DNA. The gene encoding $PutA_{669}$ was engineered as previously described and was cloned into a pET23b vector for expression as a C-terminus hexahistidine tag protein (*29*). *E. coli* strain BL21 DE3 pLysS (Novagen) was used as the host for the expression of $PutA_{669}$-$(His)_6$. *E. coli* strain JT31 *putA*$^-$ was a generous gift from J. Wood (University of Guelph, Guelph, ON). *put* intergenic DNA (419 bp) was prepared as previously described using genomic DNA from *E. coli* strain JT31 (*27*).

Preparation and Characterization of $PutA_{669}$. A truncated PutA protein containing the first 669 residues ($PutA_{669}$) was purified with a C-terminal hexahistidine tag [$PutA_{669}$-$(His)_6$] by Ni^{2+} NTA affinity chromatography (Novagen) as previously described (*29*). The C-terminal hexahistidine tag was retained after purification. Thus, in all of our experiments $PutA_{669}$ contains a C-terminal hexahistidine tag. Because $PutA_{669}$ was significantly devoid of FAD after purification on the Ni^{2+} affinity column, $PutA_{669}$ was incubated with a 10-fold molar excess of FAD overnight at 4 °C. After reconstitution of $PutA_{669}$ with FAD, unbound FAD was removed from $PutA_{669}$ first by overnight dialysis and then by applying the $PutA_{669}$−FAD mixture to a Bio-Gel P-6 column (Bio-Rad) equilibrated with 70 mM Tris (pH 7.5) containing 2 mM EDTA and 10% glycerol. The concentration of $PutA_{669}$ was determined spectrophotometrically with a molar extinction coefficient at 451 nm (see later) and by using the BCA method (Pierce) with bovine serum albumin as the standard. The molar extinction coefficient at 451 nm for FAD bound to $PutA_{669}$ in 0.1 M potassium phosphate (pH 7.0) was determined using a method described previously (*31*, *32*). The molar extinction coefficient measurements were performed three times to give an average value and a standard deviation. To determine the molar ratio of FAD to polypeptide, $PutA_{669}$ was denatured in 6 M guanidinium chloride, and the spectrum was recorded from 600 to 250 nm. The total amount of $PutA_{669}$ polypeptide was determined using the predicted molar extinction coefficient

of 73435 M^{-1} cm^{-1} at 276 nm for denatured $PutA_{669}$ and the molar extinction coefficient for uncomplexed FAD in guanidinium chloride of 11800 cm^{-1} M^{-1} at 450 nm. The contribution of FAD to the absorption at 276 nm of the denatured $PutA_{669}$ polypeptide was subtracted from the spectrum prior to the calculations using an equal molar concentration of unbound FAD. The molar ratio of FAD to the $PutA_{669}$ polypeptide was also estimated by comparing the $PutA_{669}$ concentration determined spectrophotometrically at 451 nm and by the BCA method. Activity assays for $PutA_{669}$ were performed as described previously for PutA (*9*, *12*, *25*). PDH activity was measured by using the proline:DCPIP oxidoreductase activity assay, and P5CDH activity was evaluated by monitoring reduction of NAD^+ at 340 nm. One unit of proline dehydrogenase activity is the quantity of enzyme that transfers electrons from 1 μmol of proline to dichlorophenolindophenol (DCPIP)/min at 25 °C.

To determine the K_m for FAD binding to apo-$PutA_{669}$, proline:DCPIP oxidoreductase assays were performed with apo-$PutA_{669}$ in 50 mM Tris (pH 7.5) at 25 °C in the presence of increasing FAD concentrations (0.1−2 μM). Because we observed FAD dissociated on the Ni^{2+} affinity NTA column, apo-$PutA_{669}$ was obtained directly from the Ni^{2+} affinity NTA column purification step. After the Ni^{2+} affinity NTA column, apo-$PutA_{669}$ was dialyzed overnight at 4 °C in 70 mM Tris (pH 7.5) containing 2 mM EDTA and 10% glycerol and was used immediately. Apo-$PutA_{669}$ prepared by this method was estimated to have <1% bound FAD.

Estimation of the molecular mass of $PutA_{669}$ by size exclusion chromatography was performed on a Superose 6 column (Sigma) at 4 °C that had been calibrated using the molecular mass standards carbonic anhydrase (29 kDa), bovine serum albumin (66 kDa), alcohol dehydrogenase (150 kDa), β-amylase (200 kDa), apoferritin (443 kDa), and blue dextran.

Potentiometric Titrations. Potentiometric measurements were performed as previously described under an argon atmosphere using a three-electrode single compartment spectroelectrochemical cell containing a gold wire working electrode, a silver/silver chloride reference electrode, and a silver wire counter electrode (*27*, *33*). The UV−visible spectra in each experiment were recorded on a Cary 100 spectrophotometer. Potentiometric titrations of $PutA_{669}$ were performed at 25 °C under different pH conditions in solutions containing methyl viologen (0.1 mM) and ferrocyanide (0.1 mM) as mediator dyes and pyocyanine ($E_m = -0.04$ V, pH 7.5) (5 μM) and indigo disulfonate ($E_m = -0.109$ V, pH 7.5) (2−5 μM) as indicator dyes. The $PutA_{669}$ concentrations were ~20 μM in the potentiometric experiments. The buffers used for the different pH conditions were 50 mM potassium phosphate (pH 6.5−7.5), 50 mM Tris (pH 8.0−8.5), and 50 mM sodium pyrophosphate (pH 9.0). To obtain clean spectra of $PutA_{669}$-$(His)_6$ in the potentiometric experiments, spectra of the mediator and indicator dyes were obtained in the absence of protein at the same measured potentials. The dye spectra were then subtracted from the spectra of the protein sample at each measured potential. The absorbance at 451 nm was used to monitor the amount of oxidized and reduced FAD. Equilibrium of the system in the potentiometric experiments was considered to be obtained when the measured potential drift was less than 1 mV in 5 min; this was typically 1−2 h. To ensure the system was reversible and at equilibrium, the solution was coulometrically reoxidized during the potentiometric experiments. All potential values are reported relative to the standard hydrogen electrode and were determined in the reductive direction. The reduction potentials (E_m) and n values were calculated from the Nernst equation (eq 1) where E is the measured

$$E = E_m + (0.059/n)\log([ox]/[red]) \quad (1)$$

equilibrium potential at each point in the titration and n is the number of electrons transferred. All reduction potentials exhibited Nernstian behavior as indicated by their n values.

Gel Shift Analysis. The binding of $PutA_{669}$ to *put* control intergenic DNA was measured by nondenaturing gel mobility shift assays. $PutA_{669}$ (0−600 nM) was incubated with 1 nM *put* control intergenic DNA in a total volume of 25 μL in 70 mM Tris (pH 7.5) containing 10% glycerol and 2 mM EDTA for 20 min prior to electrophoresis. Calf thymus competitor DNA (100 μg/mL) was added to the binding mixtures to prevent nonspecific $PutA_{669}$−DNA interactions. The *put* intergenic DNA (419 bp) was labeled at the 5′ end with [γ-^{32}P]ATP using a labeling protocol from Promega. As a control and for comparison, binding reactions were also performed with PutA (600 nM) under identical conditions. The $PutA_{669}$−DNA and PutA−DNA-binding mixtures were electrophoresed for 5 h at 4 °C in a agarose/polyacrylamide (0.5%/3%) nondenaturing gel in Tris−borate buffer (89 mM Tris, 89 mM boric acid, and 2.5 mM EDTA) at a constant voltage of 7 V/cm. Previously, poorly resolved PutA−DNA complexes were observed in gel shift assays using 3.5% polyacrylamide; however, a combination of agarose (0.5%) and polyacrylamide (3%) was found to provide a gel matrix that improved the resolution of the PutA−DNA complexes (*12*, *27*). After electrophoresis, the gels were analyzed by a Storm 820 phosphoimager (Molecular Dynamics). When ϕX174 ladder DNA was included in the gel, the gel was first stained with ethidium bromide and imaged using a Kodak Imaging Station 440CF. The overall dissociation constant of oxidized $PutA_{669}$ with the *put* intergenic DNA was determined as previously described by following the disappearance of the uncomplexed DNA band (*27*). $PutA_{669}$ (10 μg) and PutA (10 μg) were also applied to a separate native agarose/polyacrylamide (0.5%/3%) gel and stained with Coomassie Blue G-250 to confirm their migration in the gel shift assays.

Membrane Association Assays. Functional membrane association assays with $PutA_{669}$ and PutA were performed in 20 mM MOPS (pH 7.5) containing 10 mM $MgCl_2$ and 10% glycerol (*9*, *10*). Inverted *E. coli* strain JT31 *putA*$^-$ membrane vesicles were prepared as described by Abrahamson et al. (*9*), frozen in liquid N_2, and stored at − 70 °C until needed. $PutA_{669}$ (0.2 mg/mL) and PutA (0.2 mg/mL) were incubated with 60 mM proline, 4 mM *o*-aminobenzaldehyde, and inverted membrane vesicles from *E. coli* strain JT31 *putA*$^-$ (0.22 mg/mL membrane protein) at 25 °C in a 3 mL reaction volume. The time courses of the reactions were determined by following the formation of a yellow complex between P5C and *o*-aminobenzaldehdye at 443 nm ($\epsilon = 2590$ M^{-1} cm^{-1}) (*34*). One unit of activity is the quantity of membrane vesicles that generates 1 μmol of the chromo-

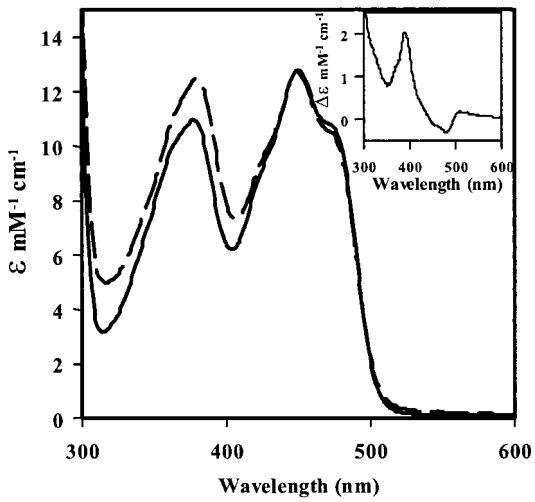

FIGURE 1: UV−visible spectra of $PutA_{669}$ and PutA. Purified $PutA_{669}$ (89.8 μM) spectrum (—) and purified PutA (67.3 μM) spectrum (---). The inset shows a difference spectrum generated by subtracting the spectrum of $PutA_{669}$ from the PutA spectrum.

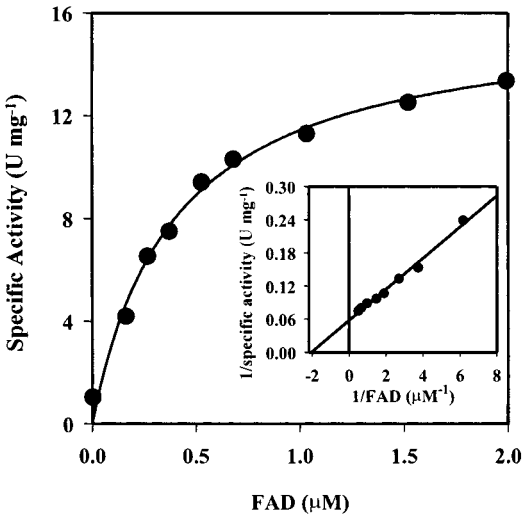

FIGURE 2: Determination of the K_m for FAD in $PutA_{669}$. PDH activity of $PutA_{669}$ was measured as a function of increasing FAD concentration. The solid line is a fit of the data obtained by nonlinear regression to the Michaelis−Menten equation. The kinetic parameters determined were $K_m = 0.40 \pm 0.04$ μM and $V_{max} = 16.0 \pm 0.6$ units/mg. The inset is a Lineweaver−Burk plot of the data with estimates of $K_m = 0.48$ μM and $V_{max} = 17.3$ units/mg.

genic complex/min at 25 °C (*9*). The functional association of $PutA_{669}$ and PutA with JT31 membrane vesicles was also characterized by using a fluorescence assay to detect active proton translocation by the electron transport chain (*9*). In a 3 mL reaction volume, $PutA_{669}$ (1 mg/mL) or PutA (1 mg/mL) was incubated for 10 min with *E. coli* strain JT31 membrane vesicles (0.11 mg/mL of membrane protein) and 9-aminoacridine (10 μM) in air-saturated 10 mM MOPS (pH 7.5) containing 10 mM $MgCl_2$ and 10% glycerol. Proline (60 mM final concentration) was then added, and the fluorescence quenching of the pH-sensitive 9-aminoacridine at 500 nm (excitation wavelength of 420 nm) was measured for 10 min at 25 °C using a Fluoromax-3 Jobin Yvon Horiba spectrofluorometer. Physical membrane association assays with PutA and $PutA_{669}$ were performed as previously described using *E. coli* strain JT31 membrane vesicles (*25*).

RESULTS

$PutA_{669}$ Properties. $PutA_{669}$ was purified from *E. coli* strain BL21 pLysS in the apoenzyme form using a protocol as previously described (*29*). Reconstitution of apo-$PutA_{669}$with FAD was achieved by overnight dialysis at 4 °C to yield $PutA_{669}$ holoenzyme. The UV−visible spectrum of reconstituted $PutA_{669}$ has absorption maxima at 278, 381, and 451 with 278/451 and 451/381 ratios of 9.7 and 1.15, respectively (Figure 1). The difference spectrum between PutA and $PutA_{669}$ shows that $PutA_{669}$ has a higher 451/381 ratio compared to PutA (1.05) (Figure 1, inset) (*25*). The molar extinction coefficient for FAD in $PutA_{669}$ was determined to be 12.8 ± 0.2 mM^{-1} cm^{-1} similar to PutA (12.7 mM^{-1} cm^{-1}) (*25*). On the basis of the denatured protein absorbance at 278 nm and the amount of released FAD, $PutA_{669}$ contains 0.8 mol of FAD/mol of polypeptide. A 0.8−0.85 molar ratio of FAD to $PutA_{669}$ polypeptide was also estimated by comparing protein quantitation using the BCA method and the molar extinction coefficient of FAD in $PutA_{669}$. PutA was reported to have a molar ratio of 0.8−0.85 mol of FAD/mol of polypeptide (*12*, *25*, *27*).

Proline:DCPIP oxidoreductase assays demonstrated that $PutA_{669}$ contains the PDH domain of PutA as anticipated. The PDH specific activity of $PutA_{669}$ was typically between 10 and 12 units/mg. Only 10% of the PDH activity was lost after $PutA_{669}$ was stored at 25 °C for 1 week. Interestingly, the PDH specific activity of $PutA_{669}$ is about 4-fold higher than the PDH specific activity of PutA (~2.5 units/mg) (*27*). No P5CDH activity was detected for $PutA_{669}$, demonstrating that the PDH and P5CDH domains were successfully separated. The K_m and V_{max} parameters of $PutA_{669}$ for proline were determined by nonlinear regression analysis of reaction velocity versus substrate concentration using the Michaelis−Menten equation. The K_m and k_{cat} values determined for $PutA_{669}$ were 102 mM and 16 s^{-1}, respectively. In identical experiments, we determined K_m and k_{cat} values for PutA of 100 mM and 7.5 s^{-1}. Thus, a smaller size and a higher catalytic turnover number for $PutA_{669}$ contribute to its 4-fold enhancement in PDH specific activity. K_m values reported from previous PutA steady-state kinetic studies were 105 mM for PutA from *E. coli* and 50 mM for PutA from *S. typhimurium* (*3*, *10*). In *E. coli*, the apparent affinity of PutA for proline increases by more than 20-fold upon PutA association with the membrane. The K_m for proline in the presence of membrane vesicles was reported to be 4.3 mM for PutA (*10*). In contrast to PutA, we observed no substantial decrease in the K_m (~80 mM) of $PutA_{669}$ for proline in the presence of membrane vesicles.

To assess the apparent FAD-binding affinity to $PutA_{669}$, the K_m of $PutA_{669}$ apoenzyme for FAD was determined by measuring the dependence of PDH activity on increasing FAD concentration as previously described for PutA (*25*). Figure 2 shows increasing PDH activity upon the addition of FAD to $PutA_{669}$ apoenzyme, indicating the formation of active $PutA_{669}$ holoenzyme. From regression analysis of the plot of reaction velocity versus FAD concentration, K_m and k_{cat} parameters of 0.40 ± 0.04 μM and 19.2 ± 0.1 s^{-1} were estimated for $PutA_{669}$. The steady-state parameters derived from a Lineweaver−Burk plot were similar with K_m and V_{max} values of 0.48 μM and 22 s^{-1} (Figure 2, inset). The K_m value of PutA apoenzyme for FAD is 0.15 μM (pH 7.5); thus the

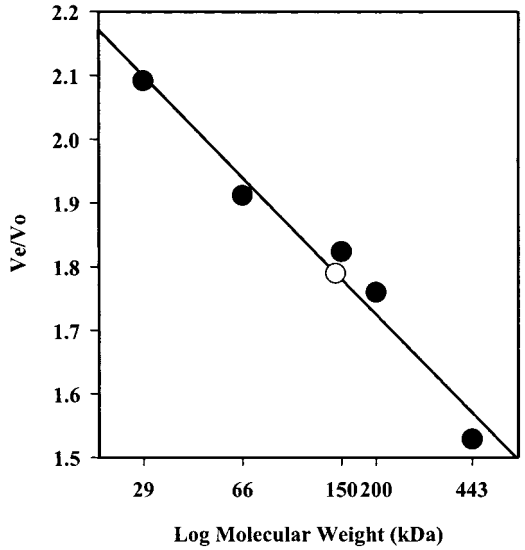

FIGURE 3: Molecular mass estimation of $PutA_{669}$. The molecular mass of $PutA_{669}$ was estimated by size exclusion chromatography (Superose 6) in 70 mM Tris (pH 7.5). The elution volumes of five standard proteins of known size were determined to generate a plot of V_e/V_o versus log molecular mass (solid circles). A molecular mass of 143 kDa was then estimated for $PutA_{669}$ (open circle) from a linear regression of the data after the elution volume of $PutA_{669}$ was determined ($V_e/V_o = 1.79$). Standard proteins used to calibrate the column were carbonic anhydrase (29 kDa), bovine serum albumin (66 kDa), alcohol dehydrogenase (150 kDa), β-amylase (200 kDa), apoferritin (443 kDa), and blue dextrin.

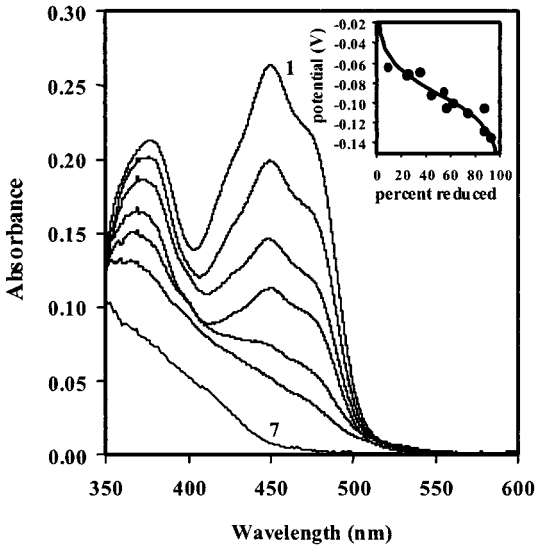

FIGURE 4: Potentiometric titration of FAD in $PutA_{669}$ (20.4 μM) in 50 mM potassium phosphate buffer (pH 7.5) at 25 °C (curves 1−7, fully oxidized, −0.072, −0.092, −0.105, −0.111, and −0.128 V, and fully reduced, respectively). The inset is a plot of measured reduction potential versus percent reduced FAD in $PutA_{669}$ fit to a theoretical curve generated from a Nernst equation for one redox center with a reduction potential of −0.091 V ($n = 2$).

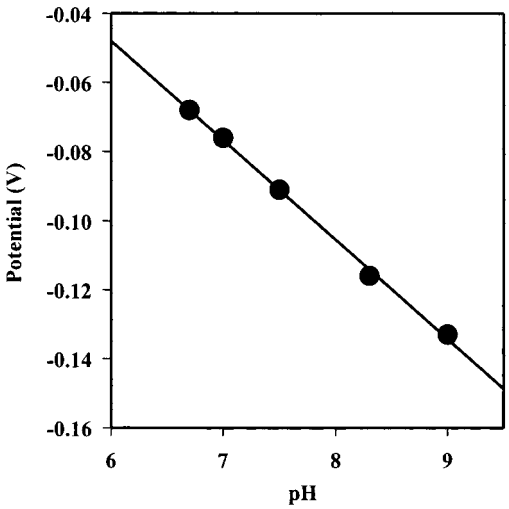

FIGURE 5: pH dependence of the reduction potential values for FAD in $PutA_{669}$ at 25 °C. Linear regression analysis of a plot of the $PutA_{669}$ reduction potential versus pH generates a slope of −0.03 V/pH unit or one proton per two-electron dependence.

apparent affinity of FAD to $PutA_{669}$ is slightly less by about 3-fold (*25*).

The PutA polypeptide has a predicted molecular mass of 143.8 kDa and purifies as a homodimer with an apparent molecular mass of 293 kDa (*12*). To test whether $PutA_{669}$ also purifies as a dimer, the oligomeric state of $PutA_{669}$ was analyzed by size exclusion chromatography. Figure 3 shows the molecular mass of $PutA_{669}$ is estimated to be 143 kDa on the basis of its behavior on the size exclusion column. Because the predicted molecular mass of the $PutA_{669}$ polypeptide is 76.1 kDa, $PutA_{669}$ appears to purify as a dimer, similar to PutA. Thus, $PutA_{669}$ contains the domain necessary for the formation of the PutA homodimer.

Potentiometric Titrations of $PutA_{669}$. Coulometric reduction of $PutA_{669}$ showed that less than 20% of the bound FAD was stabilized as the red anionic semiquinone species. This is similar to the behavior observed with PutA during a coulometric reduction. Electrochemically reduced $PutA_{669}$ was fully reoxidized ($t_{1/2} \sim 5$ min) upon the addition of an equal volume of air-saturated buffer. In contrast, complete oxidation of proline-reduced $PutA_{669}$ under the same conditions occurred more slowly ($t_{1/2} \sim 20$ min). Figure 4 shows a potentiometric titration of $PutA_{669}$ at pH 7.5 in which no stabilization of semiquinone species was observed. From a plot of measured potential versus percent reduced FAD (Figure 4, inset,) a reduction potential of −0.091 V was determined for FAD bound to $PutA_{669}$ at pH 7.5. A Nernst plot gave a slope of 0.035 V, which is near the theoretical value of 0.028 V for a $2e^-$ reduction. The E_m for $PutA_{669}$ is 15 mV more negative than the E_m for PutA ($E_m = -0.076$ V, pH 7.5) which translates into a Gibbs free energy difference of ∼0.69 kcal mol^{-1} (*27*). Because the reduction potential of enzyme-bound FAD is controlled by the binding affinity of FAD to the enzyme, the more negative reduction potential for $PutA_{669}$ indicates that the binding of reduced FAD to $PutA_{669}$ is slightly weaker than the binding of reduced FAD to PutA.

To determine the number of protons transferred per electron upon reduction of the FAD in $PutA_{669}$, potentiometric titrations were performed at different pH values within the pH range of 6.5−9.0. At pH values below 6.5, the stability of $PutA_{669}$ diminished, and at pH values above pH 9.0, dissociation of FAD from $PutA_{669}$ was observed. At all pH values, no stabilization of semiquinone species was evident. Figure 5 shows the reduction potential versus pH behavior for $PutA_{669}$. Using linear regression analysis, as shown in Figure 5, a pH dependence of 0.03 V potential/pH unit was observed for $PutA_{669}$. This is consistent with one proton transferred per two electrons transferred during reduction of FAD bound to $PutA_{669}$ as shown in the following

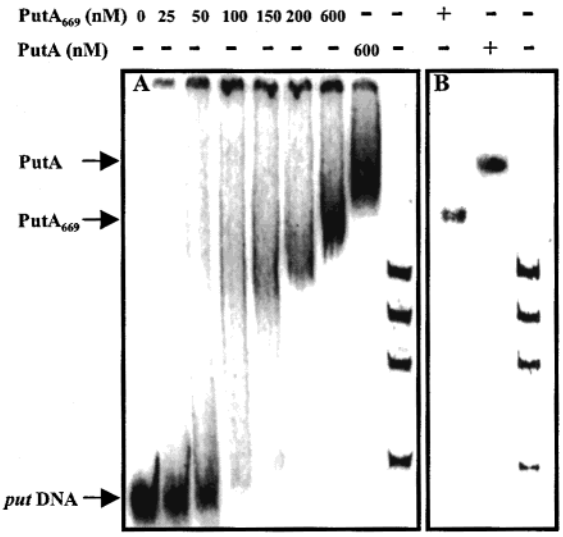

FIGURE 6: Gel mobility shift assays of *put* intergenic DNA complexed with $PutA_{669}$. (A) Gel shift assay in which increasing concentrations of $PutA_{669}$ (0−600 nM) were added to binding reactions in 70 mM Tris buffer (pH 7.5) containing *put* intergenic DNA (1 nM) and nonspecific calf thymus DNA (100 μg/mL) at 20 °C. To compare the mobility of $PutA_{669}$ and PutA−DNA complexes, PutA (600 nM) was incubated with *put* intergenic DNA (1 nM) and nonspecific calf thymus DNA (100 μg/mL) at 20 °C in a separate binding mixture. The complexes were separated using an agarose/polyacrylamide (0.5%/3%) native gel at 4 °C. As a reference, the migration of ϕX174 ladder DNA (500 ng) is shown in the last lane of the gel with molecular size standards of 1.353 kB, 1.078 kB, 0.872 kB, and 0.603 kB. (B) Migration of native $PutA_{669}$ (10 μg) and PutA (10 μg) at 4 °C in an agarose/polyacrylamide (0.5%/3%) gel. The gel was stained with Coomassie Blue and ethidium bromide to visualize the $PutA_{669}$ and PutA native bands and the ϕX174 ladder DNA (500 ng), respectively.

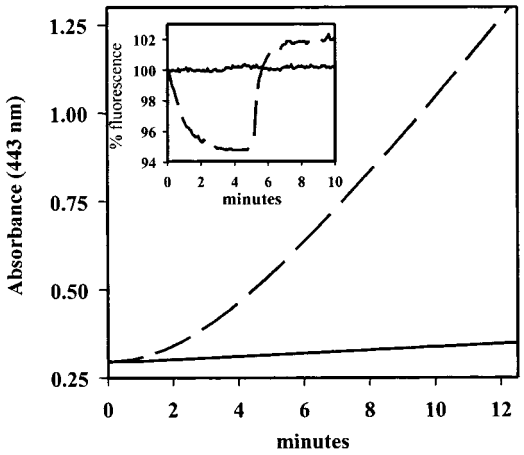

FIGURE 7: Functional membrane association assays. $PutA_{669}$ (0.2 mg/mL) and PutA (0.2 mg/mL) were incubated with 60 mM proline, 4 mM *o*-aminobenzaldehyde, and inverted membrane vesicles from *E. coli* strain JT31 *putA*$^-$ (0.22 mg/mL membrane protein) in 20 mM Mops buffer (pH 7.5) at 25 °C. The reactions were monitored at 443 nm to determine the PDH activity of $PutA_{669}$ (—) and PutA (---). The calculated specific PDH activities of $PutA_{669}$ and PutA in the above assays were 0.005 and 0.2 unit/mg of membrane protein, respectively. The inset is a fluorescence assay in which $PutA_{669}$ (1 mg/mL) and PutA (1 mg/mL) were incubated with 60 mM proline, 10 μM 9-aminoacridine, and inverted JT31 membrane vesicles (0.11 mg/mL membrane protein) in 10 mM Mops buffer (pH 7.5) at 25 °C. The time course for the reactions was followed by the decrease in fluorescence emission at 520 nm (excitation wavelength at 420 nm). PutA (---) caused a 5% decrease in fluorescence while no fluorescence decrease was observed in assays with $PutA_{669}$ (—).

reduction potential for $PutA_{669}$ measured at pH 7.0:

$$E{-}FAD_{ox} + 2e^- + H^+ \rightleftharpoons E{-}FAD_{red}H^- \qquad (2)$$

$$E_m = -0.076\ V$$

Macromolecular Associations of PutA$_{669}$. Gel shift assays were performed using the entire *put* intergenic control DNA to test whether $PutA_{669}$ contains the DNA-binding domain of PutA. Figure 6A shows a titration of the *put* control DNA with increasing amounts of $PutA_{669}$. A low-mobility protein−DNA complex formed with increasing amounts of $PutA_{669}$, demonstrating that $PutA_{669}$ binds to the *put* intergenic control DNA. The $PutA_{669}$−DNA interactions were also shown to be specific since the inclusion of nonspecific DNA in the binding reaction did not interfere with the formation of the $PutA_{669}$−DNA complex. As anticipated, the $PutA_{669}$−DNA complex displayed a greater mobility than the PutA−DNA complex in the native agarose/polyacrylamide gels (Figure 6A). The $PutA_{669}$−DNA complex migrated at a position just above the 1.3 kb marker of the ϕX174 ladder DNA. The positions of the $PutA_{669}$−DNA and PutA−DNA complexes were confirmed by native gel analysis of $PutA_{669}$ and PutA (Figure 6B). Both $PutA_{669}$ and PutA migrated as a single band in native agarose/polyacrylamide gel electrophoresis. A dissociation constant of ~15 nM was determined for oxidized $PutA_{669}$ with the *put* intergenic DNA from several gel shift assays by fitting the binding data with one independent $PutA_{669}$ binding site (data not shown). The dissociation constant for $PutA_{669}$ with the *put* intergenic DNA is about 3-fold lower than that reported for PutA (45 nM) (*27*). As observed previously with PutA, the addition of proline (30 mM) to the binding reaction did not disrupt the $PutA_{669}$−DNA interactions.

To determine whether $PutA_{669}$ can associate with the membrane, we performed functional membrane association assays. Because PutA and $PutA_{669}$ react slowly with oxygen in the presence of proline, an electron acceptor is required to achieve facile turnover of the enzyme. In the functional membrane association assay, membrane vesicles prepared from *E. coli* strain JT31 *putA*$^-$ serve as the electron acceptor. Functional association of PutA with the membrane is observed by following the formation of a yellow complex between *o*-aminobenzaldehyde and P5C, the product of the first step of proline oxidation. Figure 7 shows that PutA functionally associates with the membrane vesicles with a specific activity of 0.2 unit/mg of membrane protein. In contrast, the functional membrane association observed with $PutA_{669}$ is 40-fold lower with a specific activity of 0.005 unit/mg of membrane protein. We also assessed $PutA_{669}$ membrane associations by fluorescence assays, in which proton translocation across the membrane during electron transport is detected using the pH-sensitive fluorophore 9-aminoacridine. In a control assay with PutA, a decrease in fluorescence of 9-aminoacridine was observed (Figure 7, inset), demonstrating that electron transfer from proline to the membrane catalyzed by PutA supports proton translocation across the membrane. However, no evidence of proton translocation was detected in identical experiments with $PutA_{669}$, indicating that it does not functionally associate with the membrane. The inability of $PutA_{669}$ to associate with

membrane vesicles was also confirmed by physical membrane association assays. Brown and Wood (*25*) have shown that PutA associates with inverted membrane vesicles at a proline concentration of about 0.11 mM proline. In contrast to PutA, $PutA_{669}$ was not observed to associate with the membrane vesicles in the presence of proline (30 mM) (data not shown). Thus, it appears $PutA_{669}$ does not bind to the membrane.

DISCUSSION

The functional diversity of PutA in *E. coli* is derived from two catalytic domains and two macromolecular association domains. Previous primary structure analysis of PutA outlined the approximate locations of the PDH and P5CDH domains by using distinct PDH and P5CDH enzymes (*28*). Primary structure analysis, however, was not useful for identifying the DNA- and membrane-binding domains. Our objective was to isolate and separately characterize the PDH domain to better understand the functional organization of PutA. We sought to determine whether the DNA- and membrane-binding domains were positioned near the PDH domain. We generated a truncated form of PutA that contains only PDH activity ($PutA_{669}$) by genetically removing the P5CDH domain. So far, we have been unsuccessful at isolating and purifying a soluble and active P5CDH domain of PutA. From our current observations it appears that the P5CDH domain is not soluble apart from the PDH domain.

$PutA_{669}$ was purified as an apoprotein and was reconstituted with FAD to form a fully active PDH. Like PutA, $PutA_{669}$ purifies as a dimer, indicating that residues 1−669 are involved in stabilizing the oligomeric state of PutA. The kinetic parameters determined for $PutA_{669}$ are similar to those for PutA with a K_m value for proline of 102 mM and a catalytic turnover number for proline oxidation of $\sim 16\ s^{-1}$. A possible explanation for the slightly higher catalytic turnover number for $PutA_{669}$ may be that the electron acceptor dye has greater accessibility to the PDH active site in $PutA_{669}$ than in PutA. As a result of the lower molecular mass of $PutA_{669}$ (∼2-fold lower than PutA) and the higher catalytic turnover number (∼2-fold higher that PutA), the PDH specific activity for $PutA_{669}$ (∼10 units/mg) is 4-fold greater than for PutA (∼2.5 units/mg). The properties of FAD bound to $PutA_{669}$ were characterized by spectroscopic, kinetic, and electrochemical methods. The higher K_m value (0.4 μM) for FAD in $PutA_{669}$ indicates that the binding of oxidized FAD to the PDH active site may be weaker in $PutA_{669}$ than in PutA ($K_m = 0.15\ \mu M$). Reduced FAD also appears to bind less tightly to $PutA_{669}$, as demonstrated by the 15 mV more negative E_m value (−0.091 V, pH 7.5) for FAD in $PutA_{669}$ than in PutA (−0.076 V, pH 7.5) (*27*). It is apparent, however, that the FAD-binding environment of $PutA_{669}$ is similar to that of PutA since only small differences in their kinetic and electrochemical properties were observed. Accordingly, we conclude that residues 670−1320 do not contribute to the FAD-binding site in PutA. The pH dependence for the reduction of the FAD bound to $PutA_{669}$ shows that one proton is transferred per two electrons, indicating that bound FAD is in the anionic hydroquinone state. The pH behavior of $PutA_{669}$ will also need to be defined in the presence of substrate to test whether proline/P5C binding affects the protonation state of the reduced FAD. Spectroscopic data of proline-reduced PutA suggest that bound FAD is in the 1,5-dihydroquinone state ($FADH_2$) (*25*).

Our analysis of the macromolecular associations of $PutA_{669}$ shows that $PutA_{669}$ binds to the *put* intergenic control DNA but does not bind to membrane vesicles. We demonstrated that $PutA_{669}$ binds specifically to the *put* intergenic control DNA with a binding affinity analogous to that of PutA. Thus, we conclude that the DNA-binding domain is positioned near the PDH domain and is not in residues 670−1320 of PutA. Since PDH activity is required for the regulation of PutA macromolecular associations, it seems reasonable that the DNA-binding domain is near the PDH active site (*35*). We surmised that $PutA_{669}$ would also associate with the membrane. Muro-Paster et al. (*18*) have demonstrated that DNA binding and membrane binding in PutA are mutually exclusive, implying that the DNA- and membrane-binding domains are in close proximity. Furthermore, the PDH domain needs to be properly positioned with the membrane to catalyze the transfer of two electrons from proline to an acceptor in the electron-transport chain. Thus, we were surprised to observe that $PutA_{669}$ does not bind to membrane vesicles. Our results indicate that a membrane-binding domain from residues 670−1320 is required for the functional association of PutA with the membrane. Ling et al. (*28*) highlighted three hydrophobic regions in PutA (residues 160−170, 770−820, and 1205−1220) as possible membrane-binding motifs. It is conceivable then that PutA requires more than one membrane-binding domain to peripherally associate with the membrane. Therefore, the failure of $PutA_{669}$ to bind to the membrane does not necessarily signify that residues 1−669 are devoid of a membrane-binding domain. It may just indicate that without a second membrane-binding domain from residues 670−1320 the $PutA_{669}$−membrane interactions are too weak to form a stable association.

Developing structure−function relationships for the multifunctional PutA protein is a challenging process due to its large size and lack of a three-dimensional structure. Our study is the first attempt to dissect the PutA protein and isolate smaller domains for functional analysis. Here, we generated a recombinant bifunctional PDH from the *putA* gene in *E. coli* that retains the PDH- and DNA-binding activities of PutA but lacks P5CDH activity and membrane associations. $PutA_{669}$ will be used to investigate the mechanism of proline oxidation and the regulation of PutA−DNA binding without interference from the P5CDH active site in PutA. After the $PutA_{669}$ crystal structure is solved, we anticipate exploring structure−function relationships in the PDH active site to identify key residues involved in FAD binding, proline oxidation, and DNA binding. Future work will also be directed at isolating a soluble P5CDH domain from PutA.

ACKNOWLEDGMENT

We thank Prof. Janet Wood for providing training in the preparation of membrane vesicles from *E. coli*.

REFERENCES

1. Wood, J. M. (1981) *J. Bacteriol. 146*, 895−901.
2. Menzel, R., and Roth, J. (1981) *J. Biol. Chem. 256*, 9755−9761.
3. Menzel, R., and Roth, J. (1981) *J. Biol. Chem. 256*, 9762−9766.

4. Chen, L.-M., and Maloy, S. (1991) *J. Bacteriol. 173*, 783−790.
5. Keuntje, B., Masepohl, B., and Klipp, W. (1995) *J. Bacteriol. 177*, 6432−6439.
6. Vílchez, S., Manzanera, M., and Ramos, J. L. (2000) *Appl. Environ. Microbiol. 66*, 5221−5225.
7. Straub, P. F., Reynolds, P. H. S., Althomsons, S., Valentina, M., Zhu, Y., Shearer, G., and Kohl, D. H. (1996) *Appl. Environ. Microbiol. 62*, 221−229.
8. Jiménez-Zurdo, J. I., Garcia-Rodriguez, F. M., and Toro, N. (1997) *Mol. Microbiol. 23*, 85−93.
9. Abrahamson, J. L. A., Baker, L. G., Stephenson, J. T., and Wood, J. M. (1983) *Eur. J. Biochem. 134*, 77−82.
10. Graham, S., Stephenson, J. T., and Wood, J. M. (1984) *J. Biol. Chem. 259*, 2656−2661.
11. Wood, J. (1987) *Proc. Natl. Acad. Sci. U.S.A. 84*, 373−377.
12. Brown, E., and Wood, J. M. (1992) *J. Biol. Chem. 267*, 13086−13092.
13. Surber, M. W., and Maloy, S. (1999) *Biochim. Biophys. Acta 1421*, 5−18.
14. Surber, M. W., and Maloy, S. (1998) *Arch. Biochem. Biophys. 354*, 281−287.
15. Menzel, R., and Roth, J. (1981) *J. Mol. Biol. 148*, 21−44.
16. Maloy, S., and Roth, J. R. (1983) *J. Bacteriol. 154*, 561−568.
17. Ostrovsky De Spicer, P., and Maloy, S. (1993) *Proc. Natl. Acad. Sci. U.S.A. 90*, 4295−4298.
18. Muro-Pastor, A. M., Ostrovsky, P., and Maloy, S. (1997) *J. Bacteriol. 179*, 2788−2791.
19. Chen, C. C., Tsuchiya, T., Yamane, Y., Wood, J. M., and Wilson, T. H. (1985) *J. Membr. Biol. 84*, 157−164.
20. Ostrovsky De Spicer, P., O'Brian, K., and Maloy, S. (1991) *J. Bacteriol. 173*, 211−219.
21. José Soto, M., Jiménez-Zurdo, J. I., van Dillewijn, P., and Toro, N. (2000) *J. Bacteriol. 182*, 1935−1941.
22. Charlier, D., Kholti, A., Huysveld, N., Gigot, D., Maes, D., Thai-Toong, T. L., and Glansdorff, N. (2000) *J. Mol. Biol. 302*, 411−426.
23. Penfound, T., and Foster, J. W. (1999) *J. Bacteriol. 181*, 648−655.
24. Raffaelli, N., Lorenzi, T., Mariani, P. L., Emanuelli, M., Amici, A., Ruggieri, S., and Magni, G. (1999) *J. Bacteriol. 181*, 5509−5511.
25. Brown, E. D., and Wood, J. M. (1993) *J. Biol. Chem. 268*, 8972−8979.
26. Ostrovsky, P. C., and Maloy, S. (1995) *Genes Dev. 9*, 2034−2041.
27. Becker, D. F., and Thomas, E. A. (2001) *Biochemistry 40*, 4714−4721.
28. Ling, M., Allen, S. W., and Wood, J. M. (1994) *J. Mol. Biol. 245*, 950−956.
29. Nadaraia, S., Lee, Y. H., Becker, D. F., and Tanner, J. J. (2001) *Acta Crystallogr. D57*, 1925−1927.
30. Strecker, H. J. (1957) *J. Biol. Chem. 225*, 825−834.
31. Thorpe, C., Matthews, R. G., and Williams, C. H. J. (1979) *Biochemistry 18*, 331−337.
32. Williamson, G., and Engel, P. C. (1984) *Biochem. J. 218*, 521−529.
33. Stankovich, M. T. (1980) *Anal. Biochem. 109*, 295−308.
34. Mezel, V. A., and Knox, W. E. (1976) *Anal. Biochem. 74*, 430−440.
35. Muro-Pastor, A. M., and Maloy, S. (1995) *J. Biol. Chem. 270*, 9819−9827.

BI025706F